

Article ID: 1007-4627(2009)Suppl.-0142-06

# $\phi$ Meson Production in Heavy Ion Collisions at RHIC<sup>\*</sup>

SHI Xing-hua<sup>1, 2</sup>, CHEN Jin-hui<sup>1</sup>, MA Yu-gang<sup>1</sup>, CAI Xiang-zhou<sup>1</sup>, MA Guo-liang<sup>1</sup>

(1 Shanghai Institute of Applied Physics, Chinese Academy of Sciences, Shanghai 201800, China;

2 Graduate School of Chinese Academy of Sciences, Beijing 100049, China)

**Abstract:** We present  $\phi$  meson production in Cu+Cu and Au+Au collisions measured by the STAR experiment at RHIC. The hadronic decay mode  $\phi \rightarrow K^+ K^-$  is used in the analysis. The yields for  $\phi$  meson in Cu+Cu and Au+Au collisions at a given beam energy are scaled by the number of participant. The  $N_{\text{part}}$  normalized  $\phi$  meson yields in heavy ion collisions over those from p+p collisions are larger than 1 and increase with collision energy. These results suggest that the source of enhancement of strange hadrons is related to the formation of a dense medium in high energy heavy ion collisions and can not be only due to canonical suppression of their production in smaller systems. We also present STAR results on the  $\phi$  meson elliptic flow  $v_2$  from  $\sqrt{s_{\text{NN}}} = 200$  GeV Cu+Cu at RHIC. The elliptic flow in Cu+Cu system that has the similar relative magnitude and qualitative features as that in Au+Au system. The observations imply the hot and dense matter with partonic collectivity has been formed in heavy ion collisions at RHIC. However, eccentricity normalized  $v_2$ ,  $v_2/(n_q \epsilon_{\text{part}})$  is lower for Cu+Cu than for Au+Au collisions at 200 GeV. So this might indicate thermalization has not been reached in 200 GeV Cu+Cu collisions.

**Key words:**  $\phi$  meson; production; elliptic flow

**CLC number:** O572.33      **Document code:** A

## 1 Introduction

The main goal of relativistic heavy ion collision program is to search for QCD predicted new state of matter, and study the equation of state of nuclear matter at extremely high temperature and energy density. Searching for its existence and measuring its properties will greatly enrich our knowledge about how matter and the universe are formed. Definite experiment data have been gotten in Cu+Cu and Au+Au collisions at  $\sqrt{s_{\text{NN}}} = 62$  GeV and  $\sqrt{s_{\text{NN}}} = 200$  GeV in STAR collaboration at RHIC by now. These data and results are crucial to the understanding of the properties of the produced state of new matter.

Since the discovery of the lightest vector meson  $\phi$  from the  $K^+ K^-$  channel in  $K^- p$  interactions at 2.24 GeV/c incident momentum<sup>[1]</sup>, the studies about it is an interesting and open subject.  $\phi$  meson is composed of a strange and an anti-strange quark and has hidden strangeness. And it has considerably smaller scattering cross section, then does not fully participate in the additional flow. Its life time is about 45 fm/c which is longer than the fireball lifetime. Although it is a meson, it is heavy in comparison with mesons consisting of u and d quarks, having a mass ( $m_\phi = (1\ 019.45 \pm 0.020)$  MeV/c<sup>2</sup>)<sup>[2]</sup> comparable to the proton and  $\Lambda$  baryons. So  $\phi$  meson is a good probe to the properties

\* **Received date:** 28 Aug. 2008; **Revised date:** 6 Feb. 2009

\* **Foundation item:** National Science Foundation of China(10610285, 10705043, 10705044)

**Biography:** Shi Xing-hua(1981-), female(Han Nationality), Shanghai, China, Graduate Student, working on the field of nuclear and particle physics; E-mail: shixinghua@sinap.ac.cn

of medium in heavy ion collisions at RHIC.

A comparison of the properties of  $\phi$  meson in different colliding systems and energies may help us to understand the production mechanism for the  $\phi$  meson and its interaction with other particles.

## 2 Data Set

The data in this paper are taken from the experiments performed in 2004 (Au+Au) and 2005 (Cu + Cu) using STAR's<sup>[3]</sup> Time Projection Chamber (TPC)<sup>[4]</sup> at RHIC. The TPC magnetic field is 0.5 T. The data is also taken in the reverse field configuration. Using a minimally biased trigger (MB),  $8.86 \times 10^6$  and  $1.5 \times 10^7$  events from the (0%–60%) centrality collisions of Cu + Cu at  $\sqrt{s_{NN}} = 62$  GeV and 200 GeV for getting spectra and  $2.35 \times 10^7$  events from the (0%–60%) centrality collisions at  $\sqrt{s_{NN}} = 200$  GeV for getting elliptic flow are analyzed, respectively.  $1.35 \times 10^7$  MB,  $1 \times 10^7$  events from a central trigger (0%–12%) for 200 GeV Au + Au events and  $6.2 \times 10^6$  62.4 GeV Au + Au events are also analysed. The more peripheral Cu + Cu collision data are not analyzed due to large vertex inefficiencies. The  $\phi$  meson spectra for Au + Au collisions at 200 GeV using these data set are presented elsewhere<sup>[5]</sup>. Centrality selections for the Au + Au and Cu + Cu collision utilize the uncorrected charged particle multiplicity for pseudorapidities  $|\eta| < 0.5$ , measured by the TPC.

## 3 Spectra Analysis and Results

The  $\phi$  meson yield in each transverse momentum  $p_T$  bin is extracted from the invariant mass ( $M_{inv}$ ) distributions of  $K^+ K^-$  candidates after the subtraction of combinatorial background estimated using the event mixing technique<sup>[5–7]</sup>. The charged kaons are identified through their ionization energy loss in the TPC. The drop in lower  $p_T$  is consistent with the mass peak variation of reconstructed  $\phi$  mesons embedded in real data. These are consist-

ent with the simulation values and are understood within the ambit of the detector resolution effects<sup>[8]</sup>. In these embedding simulations,  $\phi$  ( $\rightarrow K^+ K^-$ ) mesons decay and detector response are simulated within the STAR GEANT framework. The resulting simulated signals are then embedded into real events before being processed for the standard STAR event reconstruction. These data are then processed like real data and analyzed to reconstruct the embedded  $\phi$ <sup>[5, 6, 8, 9]</sup>. The embedding simulations are also used to obtain the  $\phi$  meson acceptance and tracking efficiency<sup>[8, 9]</sup>. It is found to increase from 3% at  $p_T = 0.5$  GeV/c to about 40% at  $p_T = 3$  GeV/c for central Cu + Cu collisions. The centrality dependence of these values are small for Cu + Cu collisions. At higher  $p_T$  (3–5 GeV/c) the efficiency remains constant. The final  $\phi$  meson spectra is corrected by this efficiency and acceptance, vertex finding efficiency ( $\sim 92.5\%$ ) as well as for the branching ratio of 49.2% for the channel  $\phi \rightarrow K^+ K^-$  we have studied in this analysis.

Systematic errors for the  $\phi$  production measurements in Cu + Cu collisions include: uncertainties in efficiency ( $\sim 8\%–14\%$ ); Kaon identification from  $dE/dx$  (8%); Kaon energy loss corrections ( $\sim 3\%–4\%$ ), residual background shape (4%); magnetic field configuration ( $\sim 3\%$ ). The systematic errors are added in quadrature. Systematic errors for the  $\phi$  meson spectra are similar at both energies. The total systematic errors for  $\phi$  yields at both energies are estimated to be  $\lesssim 18\%$  over the entire  $p_T$  range studied. The systematic errors discussion for Au + Au collisions can be found in Refs. [5, 6, 9]. The results are presented with statistical and systematic errors added in quadrature, unless specified otherwise.

Fig. 1 shows the  $\phi$  meson yields from Cu + Cu collisions at 62.4 and 200 GeV for  $0.4 < p_T < 5$  GeV/c and various collision centralities. The spectra are well described by the Levy function

$$\frac{d^2 N}{2\pi p_T dp_T dy} = \frac{A}{(1 + (m_T - m_\phi)/nT)^n},$$

where  $m_T = \sqrt{p_T^2 + m_\phi^2}$  and  $A$ ,  $T$ , and  $n$  are the parameters of the function. The Levy parameters  $T$

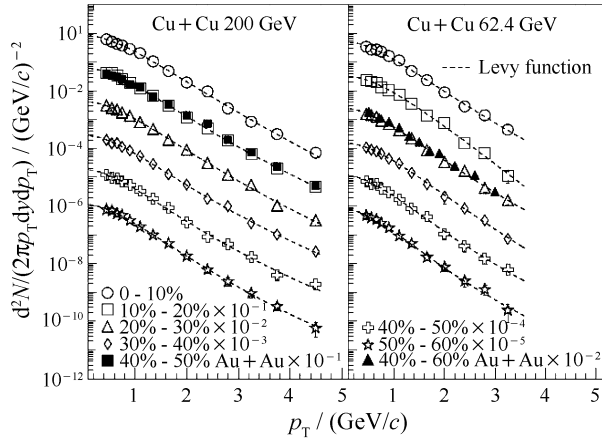


Fig. 1 Transverse momentum spectra of  $\phi$  mesons at midrapidity ( $|y| < 0.5$ ) for various collision centrality classes of Cu+Cu collisions at  $\sqrt{s_{NN}} = 62.4$  and 200 GeV. To study the system size dependence, comparison of 40%–50% Au+Au spectra to 10%–20% Cu+Cu spectra at 200 GeV and 40%–60% Au+Au spectra to 20%–30% Cu+Cu spectra at 62.4 GeV are shown because they have similar  $N_{part}$  values. The errors shown are statistical and systematic errors added in quadrature. The spectra are fitted to a Levy function.

and  $n$  have similar values for the Cu+Cu and Au+Au systems with similar number of participating nucleons  $N_{part}$  at 200 GeV. This reflects similar shape of the  $\phi$  spectra in the both collision systems at a given energy and  $N_{part}$ . The comparisons of  $\phi$  spectra between 40%–50% central Au+Au ( $N_{part} = 76.66$ ) and 10%–20% central Cu+Cu ( $N_{part} = 74.47$ ) at 200 GeV, and between 40%–60% central Au+Au ( $N_{part} = 59.90$ ) and 20%–30% central Cu+Cu ( $N_{part} = 52.27$ ) at 62.4 GeV are shown in Fig. 1. Similarity in both shape and yields are at  $\sim 10\%$  level. This is further quantified by studying their rapidity density ( $dN/dy$ ) and the average transverse momentum ( $\langle p_T \rangle$ ) for both the colliding systems.

Fig. 2 shows the  $dN/dy$  (upper panel) and  $dN/dy/N_{part}$  (middle panel) as a function of  $N_{part}$  for the two colliding systems at 200 and 62.4 GeV. The results from p+p are also presented. The 200

GeV p+p data are from STAR<sup>[7]</sup> and the 63 GeV data is from ISR<sup>[10]</sup>. The  $\phi$  production at 63 GeV reported a  $d\sigma/dy$  at  $y=0-0.33$  to be  $(0.44 \pm 0.11 \pm 0.1)$  mb. We have used the p+p inelastic

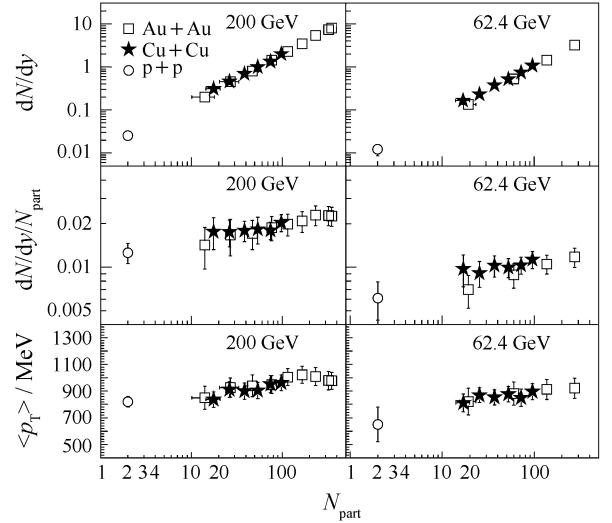


Fig. 2  $dN/dy$  at midrapidity for  $\phi$  mesons for various collision centrality classes in Cu+Cu and Au+Au at  $\sqrt{s_{NN}} = 200$  GeV and 62.4 GeV. Also shown are the results from p+p collisions. Middle panels: same as above for  $dN/dy/N_{part}$ . Lower panels: Average transverse momentum ( $\langle p_T \rangle$ ) for  $\phi$  mesons at midrapidity for various event centrality classes in Cu+Cu and Au+Au collisions at  $\sqrt{s_{NN}} = 62.4$  GeV and 200 GeV. The  $p_T$  for  $\phi$  mesons in p+p collisions are also shown. The error bars are statistical and systematic errors added in quadrature.

cross-sections of 36 and 42 mb for the beam energies of 62.4 and 200 GeV respectively. The results show both  $dN/dy$  and  $dN/dy/N_{part}$  of  $\phi$  mesons at a given energy are similar for Cu+Cu and Au+Au for collisions having similar  $N_{part}$ . The  $p_T$  of  $\phi$  mesons in Cu+Cu and Au+Au collisions are also found to be similar for collisions with similar  $N_{part}$  (Fig. 3 lower panel). From the Figure, however, We note that the  $dN/dy$  and  $p_T$  are lower for 62.4 GeV compared to 200 GeV for a given  $N_{part}$ . It will be interesting to see if such an observation is found for other produced hadrons at RHIC. The similar  $N_{part}$  dependence of  $dN/dy$  for  $\phi$  mesons in Cu+Cu and Au+Au collisions at RHIC is different from

observations at SPS and AGS<sup>[11, 12]</sup> regarding collision ion species dependence of the strange hadron production. At those lower energies, for similar  $N_{\text{part}}$  the strange hadron production is higher for smaller colliding system. The differences may be due to higher centre of mass energy at RHIC.

Upper panel in Fig. 3 shows the ratio of strange hadron production normalized by  $N_{\text{part}}$  in nucleus-nucleus collisions relative to corresponding results from  $p+p$  collisions at 200 GeV. The results are plotted as a function of  $N_{\text{part}}$ . We observe

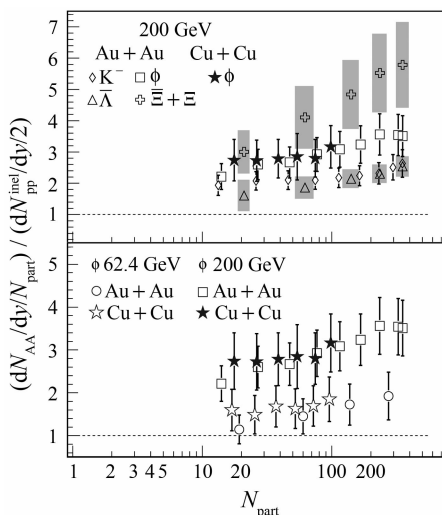


Fig. 3 Ratio of yield of  $K^-$ ,  $\phi$ ,  $\bar{\Lambda}$  and  $\Xi+\bar{\Xi}$  normalized to  $N_{\text{part}}$  in nucleus-nucleus collisions to corresponding yield in inelastic  $p+p$  collisions as a function of  $N_{\text{part}}$  at 200 GeV. Lower panel: Same as the above for  $\phi$  mesons in  $\text{Cu}+\text{Cu}$  collisions at 200 and 62.4 GeV. The  $p+p$  collision data from 200 GeV are from STAR<sup>[6]</sup> and 62.4 GeV from ISR<sup>[10]</sup>. The error bars are shown are both statistical and systematic errors added in quadrature.

the ratios for  $K^-$ <sup>[13]</sup>,  $\bar{\Lambda}$  and  $\Xi+\bar{\Xi}$ <sup>[14]</sup> show an enhancement (value  $> 1$ ) that increases with increase in the number of strange quark(s). The enhancement in these open strange hadrons increases with collision centrality and reaches its maximum at the most central collisions. The enhancement of  $\phi$  meson production from  $\text{Cu}+\text{Cu}$  and  $\text{Au}+\text{Au}$  collisions deviates from the number of strange quark ordering. They are enhanced more than  $K^-$  and  $\bar{\Lambda}$  but less compared to  $\Xi+\bar{\Xi}$ . In spite of being differ-

ent particle type (meson or baryon) and having different masses, the results for  $K^-$  and  $\bar{\Lambda}$  are very similar in the entire centrality region studied. This rules out baryon-meson effect being the reason for the deviation of  $\phi$  mesons from the number of strange quark ordering seen in Fig. 3 (upper panel). The observed deviation is also not a mass effect since the enhancement in  $\phi$  production is larger than  $\bar{\Lambda}$  (which has mass close to  $\phi$ ).

The  $\phi$  meson production due to its  $s\bar{s}$  structure is unlikely to be canonically suppressed. The observed enhancement of  $\phi$  meson production then is a clear indication of dynamical effects associated with medium density being responsible for strangeness enhancement in  $\text{Au}+\text{Au}$  collisions at 200 GeV. Further,  $\phi$  mesons do not follow the strange quark ordering as expected in the canonical picture for strange hadron production. The observed enhancement in  $\phi$  production being related to medium density is further supported by the energy dependence shown in Fig. 3 lower panel. The  $\phi$  production relative to  $p+p$  collisions is larger at higher beam energy, a trend opposite to that predicted in canonical models for other strange hadrons. Earlier measurements have indicated  $\phi$  meson production is not from coalescence of  $K\bar{K}$  and minimally affected by re-scattering effects in the medium<sup>[6]</sup>. Recent measurements indicate that  $\phi$  mesons are formed from coalescence of seemingly thermalized strange quarks<sup>[5]</sup>. All these observations put together along with the observed centrality and energy dependence of  $\phi$  meson production (shown in Fig. 3) indicates the formation of a dense medium in heavy ion collisions where strange quark production is enhanced (possible mechanism could be as discussed in Refs. [15, 16]). This in turn suggests, the observed centrality dependence of the enhancement for other strange hadrons (shown in Fig. 3) is likely related to the same dynamical effect as in the case of the  $\phi$  meson. These experimental data rule out the possibility of canonical suppression being the source of the observed

strangeness enhancement at beam energies of 200 GeV.

## 4 Elliptic Flow

Forward TPC was used to determine the reaction plane in Cu+Cu collisions because of the obvious non-flow effects. But the reaction plane is not flat after run-by-run weight corrections. Then we used shift corrections to make the reaction plane flat. The function of shift corrections is

$$\Psi' = \Psi_2 + \sum_n (-\langle \sin 2n\Psi_2 \rangle \cos 2n\Psi_2 + \langle \cos 2n\Psi_2 \rangle \sin 2n\Psi_2),$$

$$n = 1, 2, 3, 4, \dots$$

where  $\Psi_2$  is the reaction plane angle after weight corrections and  $\Psi'$  is the reaction plane angle after shift corrections<sup>[17]</sup>.

Then we applied the invariant mass method<sup>[18]</sup> to extract the elliptic flow of  $\phi$  meson. at first the number of  $K^+K^-$  pairs in each invariant-mass bin is counted, irrespective of the pair azimuth. Then  $N_{K^+K^-}(m_{\text{inv}}) = N_{\phi}(m_{\text{inv}}) + N_B(m_{\text{inv}})$ , where  $N_{\phi}$  and  $N_B$  are the two parts from  $\phi$  mesons and background, which is obtained from the fit to  $\phi$  mass peak with a Breit-Wigner plus linear background function. Breit-Wigner function is expressed as

$$\frac{dN}{dm_{\text{inv}}} = \frac{A\Gamma}{(m_{\text{inv}} - m_0)^2 + \Gamma^2/4} + B(m_{\text{inv}}),$$

where  $A$  is the area under the peak,  $\Gamma$  is the Full Width Half Maximum (FWHM) of the peak in  $\text{GeV}/c^2$ ,  $m_0$  is the resonance mass position in  $\text{GeV}/c^2$  and  $B(m_{\text{inv}})$  denotes a linear residual background function. The same-event  $v_2$  of  $K^+K^-$  pairs vs invariant mass can be described by a function

$$v_2(m_{\text{inv}}) = a(m_{\text{inv}})v_{2S} + [1 - a(m_{\text{inv}})]v_{2B}(m_{\text{inv}}),$$

where  $v_2(m_{\text{inv}})$  is the  $v_2$  of same-event  $K^+K^-$  pairs,  $v_{2S} \equiv v_{2\phi}$  is the  $v_2$  of the  $\phi$  meson,  $v_{2B}$  is the  $v_2$  of combinatorial background and  $a(m_{\text{inv}}) = N_{\phi}(m_{\text{inv}})/N_{K^+K^-}(m_{\text{inv}})$  is the ratio of  $\phi$  signal to the sum of background and  $\phi$  signal. Finally  $v_2(m_{\text{inv}})$  can be calculated by the following equation in each  $m_{\text{inv}}$  bin  $v_2(m_{\text{inv}}) = \langle \cos 2(\phi_{K^+K^-} - \Psi_2) \rangle$  where  $\phi_{K^+K^-}$  is the

azimuthal angle of the  $K^+K^-$  pair. Under the assumption that the background contribution to  $v_2(m_{\text{inv}})$  is smooth as a function of  $m_{\text{inv}}$ , a polynomial function ( $v_{2B}(m_{\text{inv}}) = p_0 + p_1 m_{\text{inv}} + p_2 m_{\text{inv}}^2$ ) is used to parameterize the background  $v_{2B}$  vs  $m_{\text{inv}}$ .  $v_{2S}$  is then obtained by fitting  $v_2$  vs  $m_{\text{inv}}$  distributions in each  $p_T$  bin, with  $v_{2S}$  being a free parameter. The  $v_{2S}$  value determined by the fit corrected for the reaction plane resolution to obtain the final  $\phi v_2$ .

Fig. 4 shows the elliptic flow of the  $\phi$  meson as a function of  $p_T$  in Cu+Cu at 200 GeV together with  $v_2$  of Ks and  $\Lambda$ . In Fig. 5 we normalize the el-

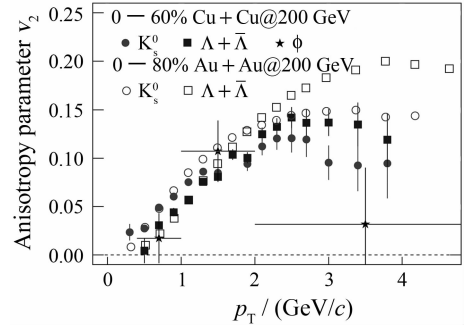


Fig. 4  $\phi$  meson  $v_2$  vs.  $p_T$  in Cu+Cu (0%–60%) and Au+Au (0%–80%) collisions at 200 GeV. And the dash line is the results from hydro model.

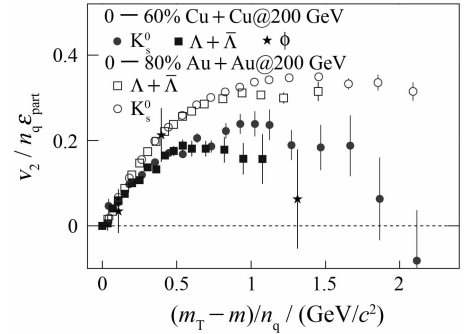


Fig. 5 The eccentricity ( $n_q \epsilon_{\text{part}}$ ) scaled  $\phi$  meson  $v_2$  vs  $p_T$  and  $m_T - m$  in Cu+Cu (0%–60%) and Au+Au (0%–80%) collisions at 200 GeV.

liptic flow  $v_2$  by the participant for different systems to remove the geometric effect. If thermalization has been reached,  $v_2/(n_q \epsilon_{\text{part}})$  should be a constant for Cu+Cu and Au+Au collisions<sup>[19]</sup>. This Figure indicates thermalization has not been reached in Cu+Cu collisions.

## 5 Conclusion

We have presented a study of the energy and system size dependence of  $\phi$  meson production using Cu+Cu and Au+Au data. These measurements provide the new experimental data showing that at a given beam energy the transverse momentum spectra in both shape and yields ( $dN/dy$ ) are similar in two colliding systems with similar  $N_{\text{part}}$ .

The enhancement in the  $\phi$  meson production is studied through the ratio of the yields normalized to  $N_{\text{part}}$  in nucleus-nucleus collisions to corresponding yields in p+p collisions as a function of  $N_{\text{part}}$ . The centrality and energy dependence of the enhancement in the  $\phi$  meson production clearly reflects the enhanced production of s-quarks in a dense medium formed in high energy heavy ion collisions. It indicates the observed enhancements in other strange hadron ( $K^-$ ,  $\bar{\Lambda}$  and  $\Xi+\bar{\Xi}$ ) production in the same collision system is likely from the same effect and not due to canonical suppression of strangeness production.

The enhancement in the  $\phi$  meson production deviates from the number of valence s-quark dependence observed for other strange hadrons. The results from  $\phi$  mesons lie in between those from single valence s-quark carrying hadrons  $K^-$  and  $\bar{\Lambda}$  and double valence s-quark carrying hadron  $\Xi+\bar{\Xi}$ . Comparisons with other strange hadron rule out the possibility of this being a baryon-meson or mass effect. The exact reason of this deviation is not clear and could be due to the effect of light-flavor valence quarks in the other strange hadrons or due to the net strangeness being zero in  $\phi$  mesons.

We also present STAR preliminary results of  $v_2$  for  $\phi$  meson from 200 GeV in Cu+Cu collisions at RHIC. FTPC tracks have been used to estimate event plane to reduce non-flow effects.  $v_2/(n_q \epsilon_{\text{part}})$  of is lower for Cu+Cu than Au+Au collisions at 200 GeV. This might indicate thermalization has not been reached in 200 GeV Cu+Cu collisions.

## References:

- [1] Bertanza L, Brisson V, Connolly P L, *et al.* Phys Rev Lett, 1962, 9: 180.
- [2] Yao W M, Amsler C, Asner D, *et al.* The Review of Particle Physics, 2006, 33: 1.
- [3] Ackerman K H, Adams N, Adler C, *et al.* Nucl Instr and Meth, 2003, A499: 624.
- [4] Anderson M, Berkovitz J, Betts W, *et al.* Nucl Instr and Meth, 2003, A499: 659.
- [5] STAR Collaboration, Abelev B I, Aggarwal M M, *et al.* ePrint: nucle-ex, 2007, 0703 033.
- [6] STAR Collaboration, Adams J, Adler C, *et al.* Phys Lett, 2005, B612: 181.
- [7] Particle Data Group, Eidelman S, Hayes K G, *et al.* Phys Lett, 2004, B592: 31.
- [8] Yamamoto E. Phi Meson Production in Au+Au Collisions at the Relativistic Heavy Ion Collider (Ph. D. thesis). Los Angeles(USA); University of California, 2001; Ma J. Measurement of Phi Meson Production and Searches for Pentaquark Particles from the STAR Experiment at RHIC (Ph. D. thesis). Los Angeles(USA); University of California, 2005; Blyth S L. Using the Phi Meson to Probe the Medium Created in Au+Au collisions at RHIC (Ph. D. thesis). Capetown (South American); University of Capetown, 2007; Chen J H. Measurement of Phi Meson Production and the Properties of Strangeness Quark from the STAR Experiment at RHIC (Ph. D. thesis). Shanghai(China); Shanghai Institute of Applied Physics, Chinese Academy of Sciences, 2007.
- [9] STAR Collaboration, Abelev B I, Aggarwal M M, *et al.* paper under preparation.
- [10] AFS Collaboration, Akesson T, Albrow M G, *et al.* Nucl Phys, 1982, B203: 27.
- [11] NA49 Collaboration, Alt C, Anticic T, *et al.* Phys Rev Lett, 2005, 96: 052 301.
- [12] E-802 Collaboration, Ahle L, Akiba Y, *et al.* Phys Rev, 1999, C60: 044 904.
- [13] STAR Collaboration, Adler C, Ahammed Z, *et al.* Phys Rev Lett, 2001, 87: 182 301.
- [14] STAR Collaboration, Adams J, Adler C, *et al.* Phys Rev Lett, 2007, 98: 062 301.
- [15] Shor A. Phys Rev Lett, 1985, 54: 1 122.
- [16] Rafelski J, Muller B. Phys Rev Lett, 1982, 48: 1 066.
- [17] Barrette J, Bellwied R, Bennett S, *et al.* Phys Rev, 1997, C56: 3 254.
- [18] Borghini N, Dinh P M, Cllitraul J Y, *et al.* Phys Rev, 2006, C70: 4 905.
- [19] Voloshin S, Poskanzer A M. Phys Lett, 2000, B414: 27.